The ontogeny of fin function during routine turns in zebrafish Danio rerio

The Journal of Experimental Biology 210, 3374-3386
Published by The Company of Biologists 2007
doi:10.1242/jeb.007484

The ontogeny of fin function during routine turns in zebrafish *Danio rerio*

Nicole Danos* and George V. Lauder

Department of Organismic and Evolutionary Biology, Harvard University, 26 Oxford Street, Cambridge, MA 02138, USA

*Author for correspondence (e-mail: ndanos@oeb.harvard.edu)

Accepted 18 July 2007

Summary

Zebrafish *Danio rerio* exhibit spontaneous, routine turns as part of their normal foraging behavior from the early free-swimming stage to adulthood. Given the importance of this behavior and its pervasiveness during zebrafish life history, the functional requirements of routine turning should play an important role in development. Conversely, the ontogeny of turning performance should reflect morphological development. In this paper we analyze the kinematics of routine turning during ontogeny in zebrafish and compare the scaling of turning kinematics to predictions from two existing models. Twenty-nine fish ranging in size from 0.38 to 1.97 cm in fork length (*FL*) were filmed at 1000 frames s^{-1} while performing routine turns. Images were analyzed using image cross-correlation to calculate body and fin velocities. We performed piecewise linear regression to identify variables that do not have a constant rate of change across ontogeny and found that two variables, turn angle and angular velocity, have a transition in slope at a body size of approximately 1 cm. Other variables show a constant positive (pectoral and caudal fin velocity, turn duration), negative (body curvature) or zero (head velocity) rate of change across ontogeny. We interpret these trends in light of morphological changes over ontogeny as well as relevant hydrodynamic conditions. We also compare the slope of the log-transformed variables to predictions from two scaling models of change in function with increasing size. We find mixed support for both models with no single model being better at predicting a single type of variable such as linear velocities. We conclude that morphological development of the paired and median fins and of the skeleton, is an important factor in determining the performance of routine turning over ontogeny. Three-dimensional kinematics and ecological behavior information will further elucidate the ontogenetic patterns observed here.

Key words: ontogeny, locomotion, scaling, *Danio rerio*.

Introduction

Fish exhibit a wide diversity of locomotor behaviors, including rapid C-start escape response (Domenici and Blake, 1997; Hale, 2002; Wakeling, 2006), linear accelerations (Tytell, 2004), steady undulatory locomotion (Jayne and Lauder, 1995; Webb, 1993) and coasting behavior inbetween locomotor bouts (McHenry and Lauder, 2005). Zebrafish (*Danio rerio* Hamilton 1822) exhibit particularly interesting locomotor diversity throughout ontogeny (Budick and O'Malley, 2000; Fuiman and Webb, 1988; Thorsen et al., 2004), which involves the behaviors mentioned above as well as a characteristic pattern of routine turning, followed by coasting, as zebrafish forage for food in the water column.

Normal locomotor behavior of zebrafish *Danio rerio* has been described across and within ontogenetic stages (Fuiman and Webb, 1988; Muller and van Leeuwen, 2003; Saint-Amant and Drapeau, 1998; Thorsen et al., 2004), and several of these studies have identified frequent turning as part of normal zebrafish locomotor behavior, distinct from escape response turns, and have termed these routine turns. Routine locomotor turns are exhibited soon after hatching and continue throughout ontogeny, despite marked developmental changes in the nervous and musculoskeletal systems. Studies of zebrafish locomotion have also been used to illuminate questions of neurological and musculoskeletal functional development as well as hydrodynamic aspects of ontogenetic trends (Drapeau et al., 2002; McHenry and Lauder, 2006; Muller and van Leeuwen, 2003; Thorsen and Hale, 2005).

Given the importance of routine turning and its pervasiveness throughout zebrafish life history, the biomechanical requirements of this behavior should play an important role in muscular, skeletal and neuronal development. Conversely, the ontogeny of turning performance as measured using kinematic metrics such as angular velocity and body curvature, should reflect underlying morphological development. Extensive knowledge of morphological development in zebrafish makes them an ideal model to study this interplay of development, functional performance and behavior: the link between morphological development and functional performance is especially clear, allowing us to make and test predictions of how one should affect the other.

While a common foraging behavior exists across ontogenetic stages, a most obvious morphological change occurs across the same stages: median and paired fins and their

associated musculature develop. The pectoral fins of zebrafish increase in area allometrically relative to body size (McHenry and Lauder, 2006) and develop complex musculature with the potential for finely tuned control of fin shape and function (Drucker and Lauder, 2003; Thorsen and Hale, 2005). The caudal, dorsal and anal fins of zebrafish as well as other species, increase isometrically in area and undergo a similar ontogenetic increase in complexity of the muscles controlling their shape and movement (Lauder and Drucker, 2004; Mabee et al., 2002; McHenry and Lauder, 2006; Standen and Lauder, 2005).

Several studies have also identified behavioral changes in fin use over ontogeny (Hale et al., 2006; Saint-Amant and Drapeau, 1998; Thorsen et al., 2004). One hypothesis that has been invoked for such changes is a change in hydrodynamic regime, from one dominated by viscous forces to one dominated by inertial forces. However, a study of coasting zebrafish has shown that at the ontogenetic stage where such behavioral transitions occur the fish still operate in a viscous regime, pointing to other causes for these behavioral shifts (Thorsen et al., 2004; McHenry and Lauder, 2005). On the other hand, functional changes such as the change in resting angle of the pectoral fins and a change in slow swimming gait, have been shown to occur at the same time as distinct morphological changes such as the expansion of muscle attachment sites on fin rays and the increase in the number of pectoral fin adductor and abductor muscles (Thorsen and Hale, 2005). We therefore expect that turning behavior, too, will be affected by morphological development of the musculoskeletal and nervous systems.

The ontogenetic stages considered here encompass a range of sizes, making size effects an important factor in zebrafish ontogeny. Various studies have modeled ontogenetic scaling effects on feeding or locomotion biomechanics (Nauen and Shadwick, 1999; Richard and Wainwright, 1995; Van Wassenbergh et al., 2005). Most of these models use systems such as the feeding apparatus of largemouth bass, which increase only in overall size and not in shape over ontogeny (e.g. Richard and Wainwright, 1995). This approach allows for the distinction between the effects of size and the effects of new morphologies on biomechanical function. Models especially relevant to our study are those that examine the scaling relationships of kinematic variables, such as maximum linear and angular velocities and accelerations, in aquatic environments (Nauen and Shadwick, 2001; Richard and Wainwright, 1995). One classic model usually invoked as a null hypothesis is by physiologist A. V. Hill (Hill, 1950). It assumes constant muscle physiological properties across size ranges but a reduced force production with increased size, due to the slower increase of muscle cross-sectional area compared to muscle mass (Hill, 1950).

In this study we describe the kinematics of routine turning across an ontogenetic range of the zebrafish *Danio rerio* that encompasses morphological, behavioral and hydrodynamic changes. We used high-speed video recordings of freely swimming zebrafish and quantified a suite of kinematic variables to describe the kinematic changes during routine turning across ontogeny. We compare the scaling coefficients from our results to the predictions from the Hill model (Hill, 1950) as well as from a model by Richard and Wainwright (Richard and Wainwright, 1995) to gain insight to the major factors determining scaling relationships of the kinematic variables that describe routine turning. We further interpret the ontogenetic patterns of kinematics and scaling in light of known morphological and hydrodynamic changes.

Materials and methods

Animals

Fish *Danio rerio* Hamilton 1822 were obtained on the day of the experiment from Tübingen wild-type lines maintained at the Zebrafish Facility of Harvard University's Molecular and Cell Biology Department. In the facility the fish were maintained at 28.5°C and on a 14 h:10 h light:dark cycle. Twenty-nine fish were filmed ranging in size (fork length, *FL*) from 0.38 to 1.97 cm. We used *FL* to describe the fish size in order to reduce errors arising from minor differences among individuals in the length of caudal fin rays. Fish sizes were obtained from digital images taken immediately after the end of the experiments.

Filming

The fish were placed in plastic Petri dishes on a stand with a Photron APX FastCam camera (1024 by 1024 pixel resolution, Photron, Inc., San Diego, CA, USA) mounted directly above. The stand did not have a solid plate for a dish base. Instead the dish rested over a circular opening approximately 1 m above the floor. The fish were illuminated with fiber optic lights from both above and below their container and were allowed to swim freely in water about 2 cm deep at room temperature (24.5°C). This depth avoided significant wall effects on the swimming fish since it was at least 5 times as deep as the fish body. We analyzed turning events only where the fish was clearly off the container bottom and where none of the body fins broke the water surface. All sequences were filmed at 1000 frames s^{-1}.

This study focused on routine turning only (Budick and O'Malley, 2000) and hence any rapid turn approaching 180° was considered an escape response and not included in the analyses.

Data analysis

We analyzed light videos using a cross-correlation analysis algorithm usually used to calculate fluid flow velocities with digital particle image velocimetry (DPIV), a routine tool in fluid dynamics studies (e.g. Drucker and Lauder, 2005; Lauder and Drucker, 2004; Standen and Lauder, 2007). In studies focused on the hydrodynamic effects of fish locomotion the fluid is typically seeded with reflective particles and then illuminated using a sheet of laser light. The cross-correlation algorithm is then applied to find the best match for the pixel intensity pattern within a rectangle of specified size between two consecutive movie frames. From the time difference between consecutive frames and the displacement and orientation changes of the pixel intensity patterns, a vector is assigned to each rectangular region. This analysis results in a two-dimensional vector field. Usually the only pattern in the images is that of the illuminated particles suspended in the fluid but in this analysis we did not seed the water with particles. Instead, as a result of our illumination, the small focus distance of the lens and the camera

light sensitivity, the fluid appears as a nearly uniform black background and the animal pigmentation is the dominant pattern of each image. Thus, the resulting vector field captures the movements of the animal's body. Since the fish body is not masked, vectors are calculated by the computer program for the entire image. Hence, there are tiny vectors throughout the image that correspond to small light changes and movement of naturally occurring particles in the water (Fig. 1), but these were ignored during our analyses and were deleted in the figures presented. Our setup required no image manipulation before this type of analysis.

To extract the magnitude and direction of the vectors we used a custom Matlab program to draw rectangles on each fin and on the head in the images of the high-speed movies with the vector field overlaid (Fig. 1); the components of the vectors enclosed in each rectangle were then saved and used to calculate kinematic variables. This process was repeated for every 10th frame. Although we had the vector fields describing the motion of the fish in almost each frame (N–1 vector fields for N frames), by looking at the movies and the resulting vectors we felt confident that we could describe the motion of the fish well by sub-sampling from our dataset.

Absolute pectoral fin speed (cm s^{-1}) is the maximum vector magnitude of all the vectors in a rectangular region on the fin tip. Since during the cross correlation analysis we used a moving window (12×12 pixels with 50% overlap) all velocity vectors were locally averaged. We therefore felt that the maximum vector in each region was a fair representation of the fin or body's performance. To obtain the speed of the pectoral fin relative to the body, we subtracted the body velocity (maximum vector magnitude in a rectangle at the base of the pectoral fins; Fig. 1, Box 5) from the absolute pectoral fin speed (the maximum vector magnitude in a rectangle around the pectoral fin tip; Fig. 1, Boxes 3 and 4). In the same way we calculated the absolute and relative speeds for both pectoral fins and for the caudal fin. We then calculated the mean speed of the right and left pectoral fins and used this mean for scaling and ontogenetic trend regressions. We calculated the absolute speed for the head and used the maximum vector magnitude (cm s^{-1}) of all the vectors enclosed by a rectangle overlaid on both eyes as the absolute head speed (Fig. 1, Box 6). Head linear velocity was used as a proxy for body linear velocity. Regressions were run on the maximum fin or head velocity magnitude of each routine turn.

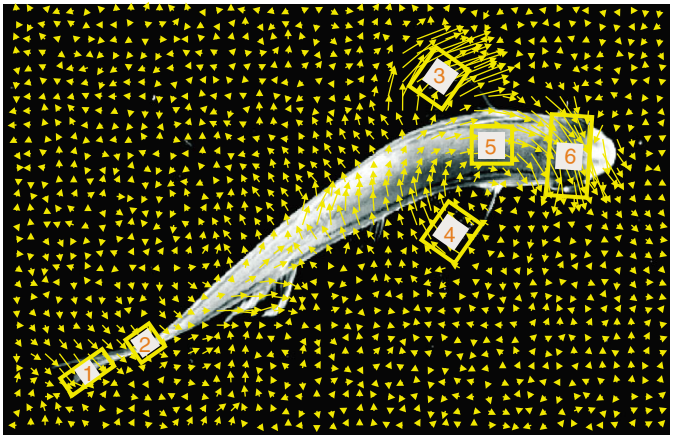

Fig. 1. Body regions tracked using Digital Particle Image Velocimetry (DPIV) cross-correlation (see text for details). Dorsal view of an adult fish (FL=3.24 cm). Yellow arrows are velocity vectors (in m s^{-1}) describing the change in position of local pixel intensity patterns between two consecutive frames (time between frames=1 ms). Arrowheads are constant size but arrow shafts are proportional to vector magnitude. Boxes: 1, tip of upper caudal fin lobe; 2, base of caudal fin; 3, left pectoral fin; 4, right pectoral fin; 5, base of pectoral fins; 6, head. Body velocities nearest to fins (boxes 2 and 5) were subtracted from fin velocities (boxes 1, 3 and 4) to obtain the velocity of the fins relative to the body.

We hypothesized that during right turns the left pectoral fin would be more active than during left turns, helping to power and control the turn, and *vice versa* for the right pectoral fin. We used pectoral fin velocity relative to body velocity, as measured above, as a measure of fin activity and assumed that the fin muscles would be active to resist hydrodynamic forces. We subtracted left pectoral fin relative velocity from right pectoral fin relative velocity, such that positive differences suggested a more active right pectoral fin while negative differences suggested a more active left fin.

Maximum turn angle is defined as the maximum angle through which the head turns for each routine turn. The orientation of the head relative to its initial position was measured from the movies in degrees (°) at 10-frame intervals. The orientation was divided by the time interval between analyzed frames (10 frames×0.001 s $frame^{-1}$) to obtain the angular velocity of the head (° s^{-1}). We were not concerned about the error associated with obtaining velocity values from displacement data (Harper and Blake, 1989), since our filming speed was relatively high (1000 frames s^{-1}) and so was our magnification (×15–20). Although we do not measure any linear velocity accelerations in this study this cross-correlation approach to image analysis would eliminate the above-mentioned types of measurement errors since it provides velocity vectors directly, without the need to first differentiate displacement data.

To calculate the mid-body curvature of the fish during turning we used a custom Matlab program. Four points along the dorsal midline were digitized on each fish: the tip of the snout, the base of the pectoral fins, halfway between the second point and the base of the tail, and at the base of the tail. The Matlab code then interpolated inbetween these four points and returned 10 evenly spaced points along the interpolated curve. For each point in each digitized frame the local curvature was calculated and from these curvature values we recorded the mean of points 4–7, those corresponding to the mid-body region. The maximum mid-body curvature during a routine turn was used in the analyses.

Turn duration was determined from graphs of turn angle and angular velocity against time for each sequence. The base of the angular velocity spike was defined as the turn start while the time at which angular velocity equaled zero and where the turn angle did not differ by more than 5° from the final turn angle was designated as the turn end.

Reynolds number Re was calculated using the formula $Re=\rho VL/\mu$, where ρ=water density at 20°C (kg m^{-3}), V=maximum head velocity per sequence (m s^{-1}), L=length of fish (m) and μ=dynamic fluid viscosity of water at 20°C (Pa s).

Turn angle prediction model

Turn angle was defined as the angle through which the head rotates during a turn (Fig. 2, γ). Our model predicts turn angles based solely on body bending. Any differences between the angle predicted by this model and the maximum turn angle measured in this experiment are interpreted as fin contribution to turn angle control.

We assume a constant body curvature along the fish length and no whole body rotation due to inertia. H and T are the location of the head (H) and the tail (T) when the fish is straight, and H′ and T′ are the locations of the head and the tail at maximum curvature (Fig. 2). The turn angle γ should equal the angle between the line segment HT (*L*) and a line perpendicular to the tangent at H′ (H′O). The complementary angle to γ, α, is equal to 90–β/2 (see Eqn 1 below). The ratio of the angle inscribed by an arc of length *L* (the length of the fish) to the total angle of a circle is equal to the ratio of the length of the arc to the circumference of the circle (see Eqn 2 below). Since α=90–β/2 (Eqn 1) and γ=90–α it follows that γ=β/2. If *K* is the body curvature, and *K*=1/*R*, where *R* is radius of curvature, it follows from Eqn 2 that γ=*LK* (Eqn 3). In summary:

$$\alpha = 90 - \gamma = 90 - \beta/2 \, . \quad (1)$$

Rearranging Eqn 1:

$$\gamma = \beta/2 \, ,$$

$$\beta/4\pi = L/2\pi R \, . \quad (2)$$

Substituting *K*=1/*R* in Eqn 2 and equating Eqn 1 and Eqn 2:

$$\gamma = LK \, . \quad (3)$$

Thus using the maximum mid-body curvature and the length of the fish we can estimate the expected turn angle.

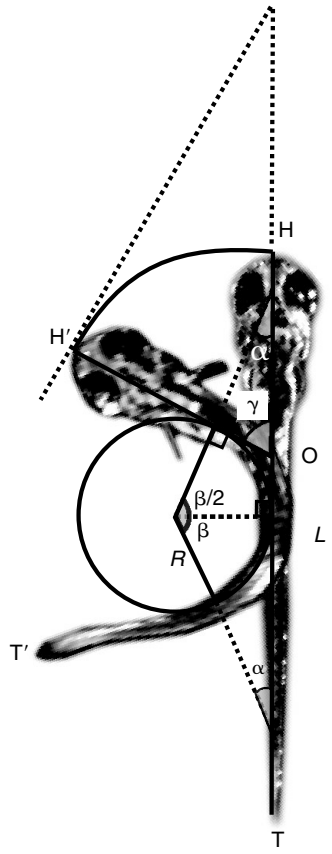

Fig. 2. A model predicting turn angle based only on midbody curvature and body length. If body bending was the only factor controlling turn angle, turn angle should equal the product of body curvature and body length (see text for more details). Curvature, *K*=1/*R*; *L*=fish length; γ=turn angle.

Statistics

When plotting kinematic variables against fork length we noticed two trends of ontogenetic change: one where the rate of change (slope) remained constant across ontogeny and a second trend where a transition existed from one rate of change to another. Based on morphological studies of the musculoskeletal system in zebrafish we predicted that this transition point would be around 1 cm total length (*TL*), when the axial, median and paired fin skeletons are fully ossified and when fin musculature has reached adult morphology.

We used ordinary least square (OLS) regressions (SigmaPlot 10, Systat Software Inc., San Jose, CA, USA) to identify the presence and value of a single transition point in the rate of change of the kinematic variables. We performed a piecewise regression with two linear segments as well as a simple linear analysis on all variables. The piecewise regression used a least squares approach to maximize the fit of two first order polynomial curves to the data, the only constraint being that the transition point had to fall within our data range. As such we did not test an *a priori* expectation for the value of the transition point. When two linear relationships are better suited for describing a dataset, the analysis of variance (ANOVA) coefficient for the transition point and the ANOVA coefficient for the entire regression has a *P*-value <0.05, and the *P*-value for a piecewise regression was smaller than the *P*-value for a simple linear regression. We used these regression methods to identify the presence of a transition point and the general range in which it was found. We were not interested in the exact value of regression slopes or the exact value of the transition point since these values can be heavily influenced by clustering of data points at the ends of the data range, but report the results of the regression nonetheless.

To determine scaling coefficients, all kinematic variables were log-transformed and regressed against the log of fork length using an OLS-ANOVA model. The slope of each regression was considered to be different from zero if the *P* value of the ANOVA was <0.05. The 95% confidence intervals (CI) were calculated and compared to the regression slopes predicted by previous scaling models (Hill, 1950; O'Reilly et al., 1993; Richard and Wainwright, 1995). We did not reject the predicted slope if our 95% CI contained the predicted slope.

Some previous studies that regressed kinematic variables against fish length have used Model II regression models (Fuiman and Webb, 1988; Hernandez, 2000; Toro et al., 2003). However, we feel that the variance in fish length due to measurement error is far smaller than the variance in kinematic variables that results from the computation of these variables. We, as well as a number of other ontogenetic scaling studies, therefore use OLS regressions in all our comparisons (McHenry

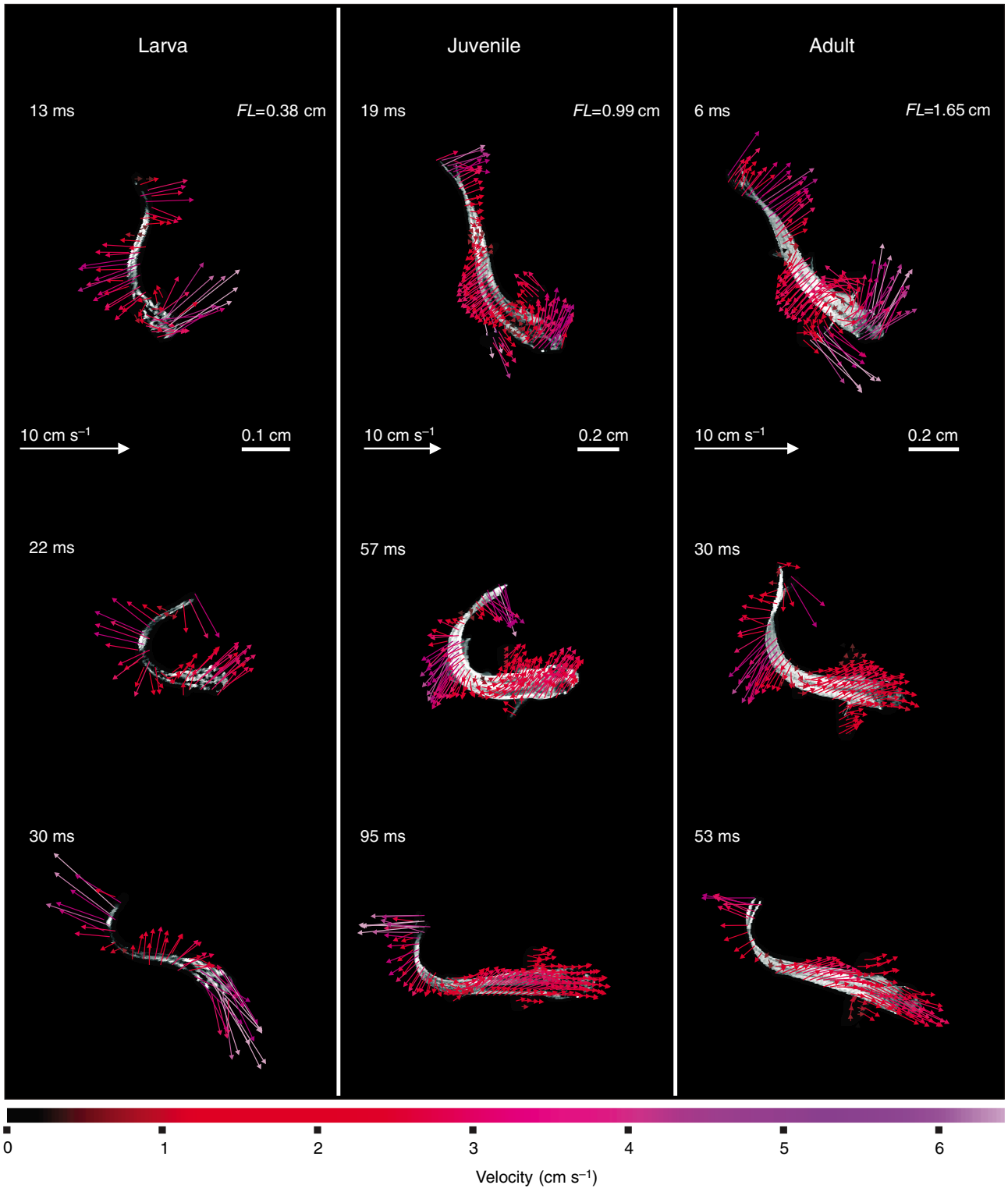

Fig. 3. Representative turning sequences across zebrafish ontogeny showing movie frames near the start, midpoint and end (top, middle and bottom rows, respectively) of each turning sequence. The first frame shown from each sequence was selected as the one where the dominant point of rotation along the body was clearly visible. The last frame selected was the frame where the head had reached its final angular displacement and the body is nearly straight. Maximum body curvature, which was usually reached near the midpoint of the turn, is largest in larvae and smallest in adults. Linear velocity of fins is greatest in adult fish even though angular velocity of the head is smallest in adults. The most prominent center of rotation for routine turns remains over the pectoral girdles in all stages examined (top row); other areas of the body may also exhibit rotational motion.

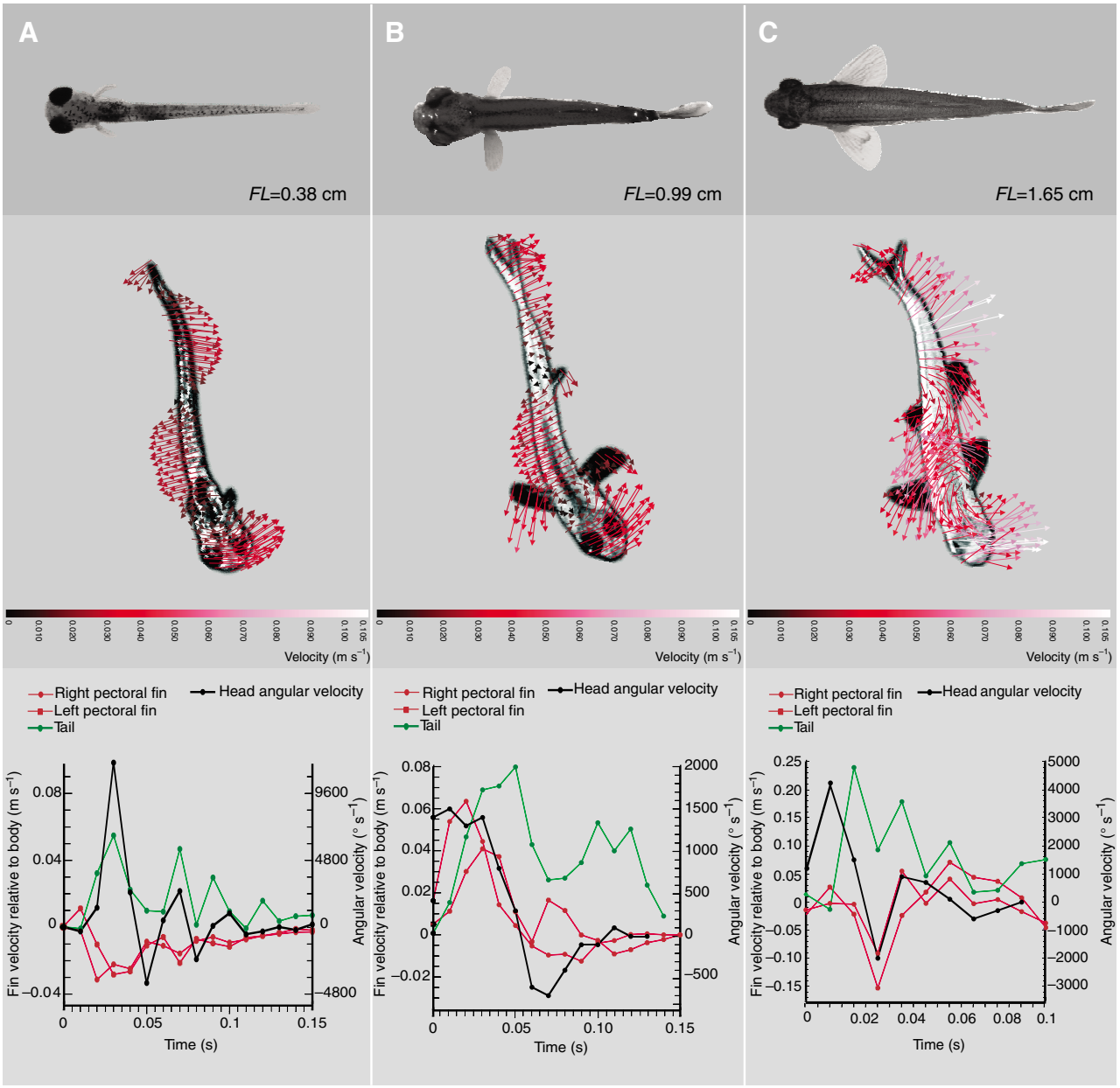

Fig. 4. Comparison of pectoral fin and tail function and their contribution to angular velocity at three sizes representative of the larval, juvenile and adult stages. Fin velocities in all three graphs are relative to body velocity (Fig. 1). Thus negative velocities indicate that the fin is moving slower than the body. (A) In the larval individual (*FL*=0.38 cm) the pectoral fins are moving more slowly than the body. The caudal fin, in contrast, is moving faster than the body and reaches its maximum linear velocity at the same time that maximum angular head velocity is reached. (B) In juvenile fish (*FL*=0.99 cm) the pectoral and caudal fins are all moving faster than the body around the time of maximum angular head velocity, suggesting that the generation of turning momentum is created by the interaction of both fin types. The caudal fin remains active longer than the pectoral fins that attain a speed close to body speed after 0.05 s, suggesting that the caudal fin is engaged in angular control later in the turn cycle as well. (C) In the adult (*FL*=1.65 cm) the fin opposite to the direction of turning is moving faster before maximum head angular velocity although the kinematic profile of adults showed very high variation.

and Lauder, 2005; Nauen and Shadwick, 1999; Richard and Wainwright, 1995).

Results

We first present routine turns from three representative individuals at distinct ontogenetic stages: larval (*FL*=0.38 cm), juvenile (*FL*=0.99 cm) and adult (*FL*=1.65 cm) in Fig. 3. For each individual we show a frame near the start, middle and end of the turn (Fig. 3). We then consider trends of ontogenetic change for body and fin kinematics (Figs 4, 5 and 6), the fit of our turn angle prediction model (Fig. 7) and the relationship between turn direction and differential pectoral fin activity (Fig. 8). Lastly we present the results of our log-transformed regressions with respect to the scaling of kinematics (Table 1).

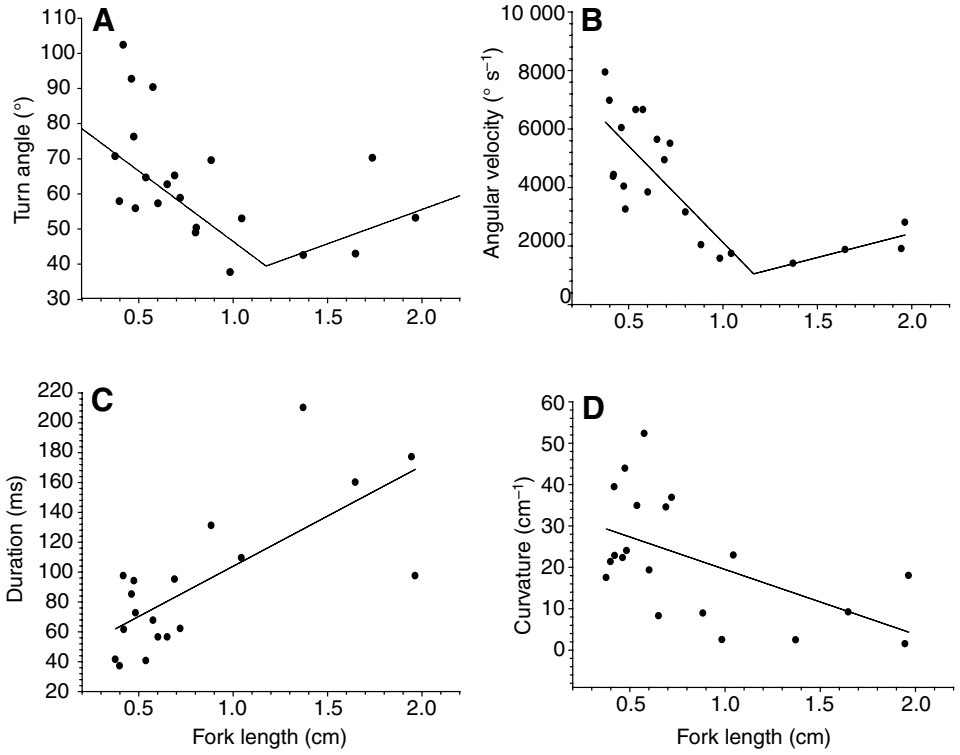

Fig. 5. Kinematic variables plotted against fork length. (A) Turn angle; (B) angular velocity; (C) duration; (D) curvature. Turn angle (A) and angular velocity (B) show a biphasic pattern of change. The transition points as identified by piecewise linear regression occur at *FL*=1.18±0.28 cm for turn angle and *FL*=1.16±0.23 cm for angular velocity. The piecewise regression for turn duration (C) against *FL*, although significant overall, did not have a significant transition point. Body curvature (D) did not have a significant piecewise regression and so we interpret the rate of change as constant across ontogeny with a slope of –16±6; a quadratic model did not fit the data significantly better than a single linear regression model. For further explanation of the regressions, see *Statistics* in Materials and methods. In all graphs each point represents the mean value per individual, from 2 or 3 turning sequences.

Within ontogenetic stage turning characteristics

Smaller fish tended to perform routine turns more often than adults. Larvae moved at overall faster body-specific speeds but similar absolute speeds (Fig. 6A), through larger angles (Fig. 5A) and at higher angular velocities (Fig. 5B) than juveniles or adults. Larvae also displayed a higher degree of lateral head movement during swimming out of the turn. As a result, in the representative final frame for a larva in Fig. 3 the turn angle appears small because the head is moving to the right while the body is traveling more towards the left. Adults, on the other hand, performed these turns less frequently and instead of exiting the turn with multiple tail beats they tended to beat their tail only once strongly to the side opposite the direction of turn and then coast to a halt. Before stopping, they typically modulated the direction and speed of coasting using their median and paired fins.

In larvae (*FL*=0.38–0.46 cm) the pectoral fins generally move more slowly than the body as indicated by the negative relative

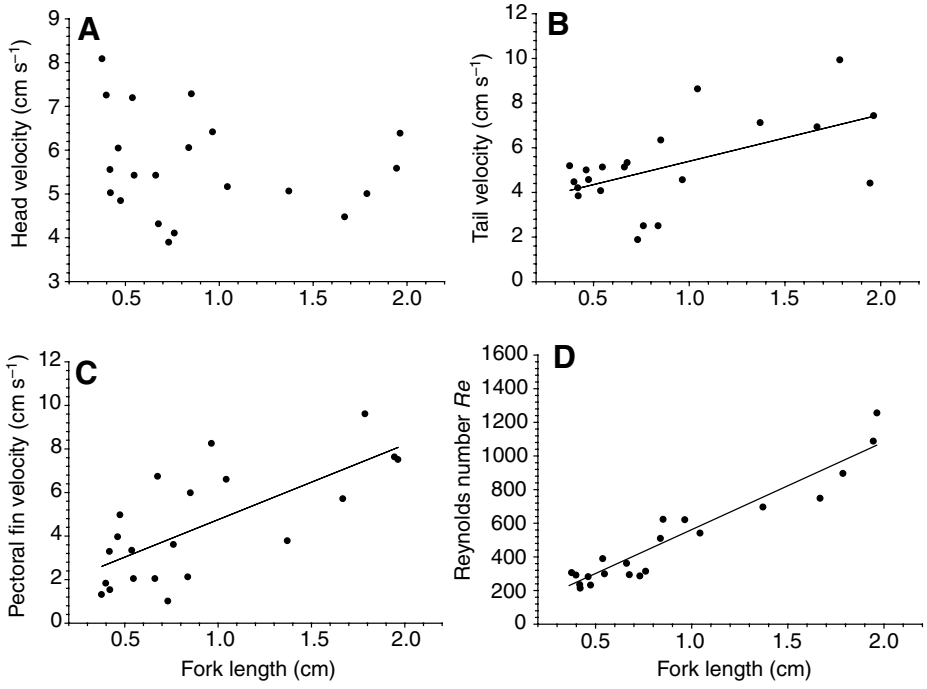

Fig. 6. Kinematic variables against fork length. (A) Head velocity; (B) tail velocity; (C) pectoral fin velocity, as the average of left and right fin velocities; (D) Reynolds number. (A) Head velocity had a slope not significantly different from zero. Tail velocity (B) increased with a slope of 3.32±1.03 and pectoral fin velocity (C) increased with a slope of 3.24±0.74. Since *Re* (D) was not measured directly but was calculated from other measured variables we did not include it in this analysis. We report the slope of its linear regression for general interest (slope=730±301). For further explanation of the regressions, see *Statistics* in Materials and methods. All graphs show mean value per individual, from 2 or 3 turning sequences.

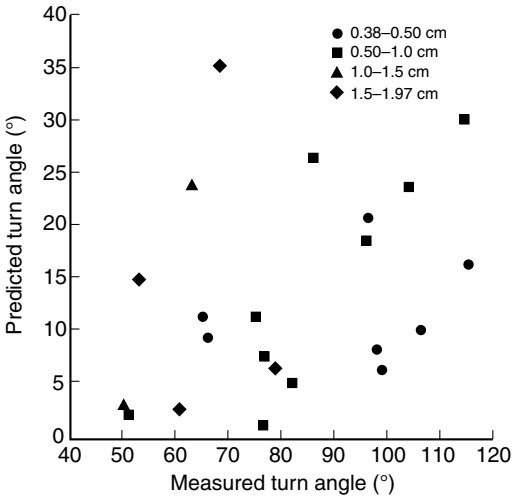

Fig. 7. Turn angles predicted by a simple model of body curvature during turning plotted against measured turning angles. The model predicts maximum turn angle to be the product of maximum body curvature (*K*) and fish fork length (*FL*), which is dimensionless. Points are coded according to *FL* (see key) and are the mean values of all turning sequences from each individual. If actual turn angles matched predicted turn angles, there should be a 1:1 relationship between the two variables. All the turn angles measured are substantially smaller than the angles predicted by the model.

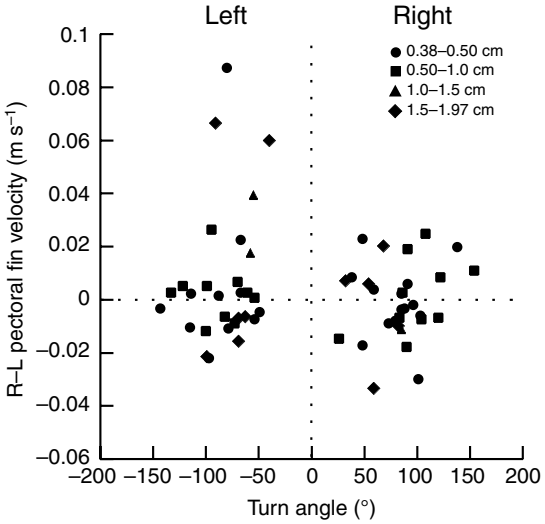

Fig. 8. Pectoral fin contribution to turn direction. The difference between right and left pectoral fin velocities, after subtraction of the body velocity, is plotted against turn angle for each sequence measured. Points are coded according to fish fork length (see key). Left turn angles are coded as negative while right turn angles are coded as positive. During a turn in either direction there is no pattern of the same fin (left or right) consistently moving faster than the other. The lack of pattern persists throughout ontogeny.

pectoral fin velocity (Fig. 4A), and are probably not actively resisting the fluid forces that result from motion through the water. For fin movement to generate turning, fin motion should coincide with body angular velocity. This timing was used as a proxy of fin contribution to turning even though we did not always observe the same sequence of fin and body action. In larvae, approximately half the time maximum pectoral fin velocity in a turn does not occur at the same time as maximum angular velocity. When the two maxima do coincide, pectoral fin velocity is usually very low, about 0.15 cm s^{-1}. However, at the same ontogenetic stage tail activity appears to follow the angular velocity of the head, even after the turn itself when the fish swims off (Fig. 4A). This close time correspondence between head angular velocity and tail velocity in larvae is a result of the increased sideways head motion during slow swimming at this ontogenetic stage.

Fish between 0.46 and 1 cm showed a more consistent pattern. Both pectoral fins had high positive relative velocities at the same time as maximum angular velocity (Fig. 4B). In small juvenile fishes the tail maximum velocity was temporally close to the maximum angular velocity and the overall tail velocity pattern closely followed the changes in angular velocity. In the example presented (Fig. 4B), tail velocity increases and decreases in accordance with angular velocity changes up to 0.09 s into the turn but then shows two spikes while angular velocity remains more or less constant. As the fish grew older the tail increasingly moved in ways that coincided less with angular velocity changes during turning.

Fish larger than 1 cm showed more variation in all variables, pectoral and caudal fin velocities relative to the body and angular velocity profiles. In the example sequence of a turning adult shown in Fig. 4C, tail movement is almost completely asynchronous with turning while the pectoral fins move with very low and even negative velocities relative to the body.

Ontogenetic distribution of kinematic variables

We find two patterns of change in kinematic variables across a size range of growing zebrafish: a biphasic pattern with two separate linear relationships and a single linear relationship between kinematic variables and size with a positive, negative or zero slope.

Turn angle (Fig. 5A) and angular velocity (Fig. 5B) show the biphasic pattern of change. Turn angle (Fig. 5A) decreased from approximately 72° to 40° near the transition point and then increased slightly to 55°. The transition point for turn angle was at *FL*=1.18±0.28 cm. Angular velocity falls from about 6200° s^{-1} to 1000° s^{-1} at *FL*=1.16±0.23 cm and then increases slightly to 2400° s^{-1} (Fig. 5B). The mean transition point for the two variables was *FL*=1.17 cm.

Turn duration, on the other hand, increases at a single linear rate from about 40 ms to 150 ms with a slope of 67±15 (Fig. 5C). Body curvature also shows a single rate of change across ontogeny, with a regression slope of –16±6 (Fig. 5D).

Head velocity does not change significantly over ontogeny (Fig. 6A). Tail and pectoral fin velocities both increase linearly (Fig. 6B,C) with a slope significantly different from zero. Tail velocity increases with a slope of 3.32±1.03 (Fig. 6B) and pectoral fin velocities with a slope of 3.24±0.74 (Fig. 6C). We did not include Reynolds number in the search for a transition point since it was not measured directly and since it describes more the hydrodynamic environment rather than the kinematics of the swimming fish. The slope of a single linear regression of Reynolds number against fork length was 730±301.

Our geometric model predicted, based on body length and

Table 1. *Regression slopes for log-transformed kinematic variables on log-fork length compared to the expected scaling coefficients from previous models*

Variable	*N*	Type	Model		OLS slope	95% CL		*P* value	R^2	Conclusion
			Hill	RW		Lower	Upper			
Head speed	20	Velocity (cm s^{-1})	0	1	–0.09	–0.25	0.07	0.30	0.06	0
Relative tail speed	22	Velocity (cm s^{-1})	0	1	0.43	0.11	0.75	0.017*	0.25	Slight positive
Relative pectoral fin speed	22	Velocity (cm s^{-1})	0	1	0.75	0.27	1.23	0.0063*	0.31	1
Maximum angular velocity	22	Angular velocity (° s^{-1})	–1	0	–0.68	–1.00	–0.37	0.0004*	0.47	–1
Maximum turn angle	22	Angle (°)	0	0	–0.32	–0.49	–0.15	0.0016*	0.40	Slight negative
Turn duration	20	Time (s)	1	0	0.57	0.26	0.88	0.0021*	0.64	Slight positive
Maximum body curvature	21	–	–	–	–0.96	–1.82	–0.10	0.041*	0.21	–1
Maximum *Re*	20	–	–	–	0.91	0.76	1.07	<0.0001*	0.87	1

N=number of individuals; up to 3 turning sequences per individual.

*Significant (P<0.05).

All statistics were calculated on $\log_{10}$-transformed variables.

Hill model: regression slopes were predicted by the geometric isometry models by Hill (Hill, 1950) and by O'Reilly et al. (O'Reilly et al., 1993), taking into account the force production capacities of increased muscle masses.

RW model: regression slopes were predicted by the geometric isometry model of Richard and Wainwright (Richard and Wainwright, 1995) based on in- and out-lever ratios determining muscle velocities.

OLS slope, ordinary least squares regression slope; lower and upper 95% CL, lower and upper limits of 95% confidence interval of the regression slope.

Conclusion summarizes the findings of this study by noting whether the regression slope confidence interval includes 0, 1 or –1. In the cases where none of these values falls within the regression slope confidence interval we describe the general trend of the slope, e.g. slight positive if the slope is significantly larger than 0 but smaller than 1.

body curvature, a range of turn angles from 0.47° to 58.36° with a mean of 13.32±1.61° (± s.e.m.). Measured maximum turn angles ranged from 26° to 154°, with a mean angle of 81.73±3.67° (± s.e.m.). All measured angles were larger than predicted (Fig. 7; only mean values per individual shown). There was no ontogenetic pattern when fish were grouped into 0.5 cm size classes.

When plotting the differential pectoral fin velocity, left fin velocity subtracted from right fin velocity, against turn angles we do not find the expected pattern of distribution (Fig. 8). We had hypothesized that the right fin would be most active (positive *y*-axis values) during left turns (negative angles) and the left fin most active during right turns. This expectation would yield a distribution pattern in the upper left and lower right quadrants of the graph. However, we see that left and right pectoral fin activity is equally distributed between positive and negative turn angles (Fig. 8).

The mode of swimming out of the turn shows a gradual ontogenetic change as well. In all the sequences recorded from zebrafish ranging in size from 0.38 cm to 0.48 cm, the fish swam for a few tail beats after the turn using alternating pectoral fin beats coordinated with axial undulations (see also Thorsen et al., 2004; Budick and O'Malley, 2000). Fishes ranging in fork length from 0.54 cm to 0.81 cm occasionally exhibited this behavior while all of the fishes above 0.89 cm used only axial undulations briefly after the turn before coasting to a stop.

Scaling

The regression results of log-transformed variables against log*FL* are presented in Table 1 and are compared to the predictions of the Richard and Wainwright (RW) and Hill models (Richard and Wainwright, 1995; Hill, 1950). The two models predict the scaling relationships of kinematic variables to body length based on different parameters. The RW model uses principles of muscle lever arm scaling while the Hill model focuses on muscle physiology scaling principles. Tail and pectoral fin absolute velocities and fin velocities relative to the body showed the same scaling relationships so we report only on relative velocities in Table 1. Different variables have different number of observations (*N*) since not all kinematic variables could be assessed for each individual fish.

Log-head velocity scaled with a slope not statistically different from zero (Table 1), matching the prediction of the Hill model. Log-relative tail velocity scaled with a positive slope significantly different from zero but smaller than 1 (Table 1). Log-relative pectoral fin velocity scaled with a significant positive slope, the 95% CI of which included 1 (Table 1), matching the prediction of the RW model.

Log-maximum angular velocity scaled with a significant negative slope (Table 1) but the 95% CI for the slope included –1 as its lower limit. Maximum turn angle also scaled with a slight negative slope, less than –1 (Table 1).

A regression of log-body curvature on log-fork length yielded a slope of –0.96 that was not significantly different from –1 (Table 1). Log-Reynolds number scaled with a slope of 0.91 (Table 1) and did not differ significantly from 1.

We find no consistent agreement between type of kinematic variable and predictive model. Linear velocity variables (head,

tail and pectoral fin velocities) did not consistently support either model. Head velocity scaled according to the Hill model predictions, while pectoral fin velocity scaled according to the RW model. Tail velocity did not support either model directly. Angular variables (angular velocity and turn angle) also differ in which model prediction they agree with. Angular velocity scales according to the Hill model while turn angle scales according to neither prediction. The models make no direct predictions about body curvature or Reynolds number.

Discussion

Budick and O'Malley found that the best way to distinguish routine from escape turns was to compare angular velocities, because routine turns always had angular velocities below 13 000° s^{-1} (Budick and O'Malley, 2000). All turns analyzed in this study had angular velocities smaller than 13 000° s^{-1} and never exceeded 180° in magnitude. We thus studied a normal part of the behavioral repertoire in developing zebrafish, which although submaximal, could have significant effects on evolutionary fitness since the behavior is exhibited continuously in food foraging and predator avoidance (Webb and Weihs, 1986).

Scaling

Previous studies of scaling in feeding salamanders and fish analyzed the effects of size change in a geometrically isometric system (Hill, 1950; O'Reilly et al., 1993; Richard and Wainwright, 1995). We used two existing models of isometric growth to predict the expected scaling coefficients of kinematics if the morphology was growing isometrically: the RW (Richard and Wainwright, 1995) and Hill (Hill, 1950) models. The models differ in the parameters they consider as determinants of kinematics. The RW model focuses on changes in muscle lever arms and predicts the effect these changes have on the scaling of kinematics. This model predicts that log-linear displacements and velocities scale against log-standard length with a slope of 1, while log-angular displacements, log-angular velocities and log-time to peak scale against log-length with a slope of zero (Table 1).

The Hill modeling approach takes into account the fact that mass increases as the cube of body length while muscle cross-sectional area, which is directly related to force production, changes with the square of body length (Hill, 1950; Nauen and Shadwick, 2001; O'Reilly et al., 1993). This approach predicts that with increased size, force production by muscles will increase at a lower rate than the body mass they need to move. It predicts log-linear displacement and log-linear velocity should scale with a slope of 1 against log-standard length. Log-angular displacement is predicted by these models to scale with a slope of 0 against log-standard length while log-time to peak variable to scale with a slope of 1 and log-angular velocity with a slope of –1 (Table 1).

Even though the locomotory morphology, such as fin area, in zebrafish does not grow isometrically (McHenry and Lauder, 2006), comparison of the scaling coefficients from our study to those from the models can still provide useful insights. Agreement of our scaling coefficients with coefficients from either one of the two isometric growth models, but not the other, can help elucidate the major determinants of scaling of kinematic variables. In these experiments it is a suite of characters and behaviors that modulate the kinematics measured, since the kinematics are of a submaximal locomotory variable and the behavior is not limited by the animal's potential (muscles are most likely not performing maximally). If the kinematics of a complex of features, components of which grow allometrically, can still scale according to a model's predictions, it could reflect the isometric nature of the functional demand instead of the isometry of the underlying morphology. In effect such a result points to a functional isometry with the negative allometry of some variables compensated by the positive allometry in others.

Head linear velocity, a proxy for body linear velocity, scaled with a coefficient of zero, as predicted by the Hill model. Angular velocity and turn duration also scaled according to the Hill model. Tail and pectoral fin linear velocities, however, showed more support for the RW model (Table 1). While body speed as measured by head velocity may be more influenced by muscle physiology changes and body muscle mass scaling, fin velocity as measured at the tip of the fin with respect to a stable site of attachment may be more influenced by changes in lever arm proportions. Hence, the assumptions of each of these models dominate the scaling of these kinematic variables and can still lead to correct scaling predictions, despite the allometric growth of other parameters or submaximal performance of active musculature.

Even experimental results from scaling studies in which isometric growth has been shown, had mixed support for the two models. The tail-flip escape response of the California spiny lobster *Panulirus interruptus* scales according to predictions based on the Hill model with the exception of angular displacement. Studies of feeding zebrafish and of running, jumping and biting lizards (allometric growth) show an even larger variation in the scaling effects of ontogeny (Hernandez, 2000; Toro et al., 2003). A study on the scaling of suction feeding in catfish identified the induction of a pressure gradient across the buccal cavity as the most important factor determining muscle force requirements, explaining the discordance between the scaling coefficients obtained experimentally and the RW and Hill predictive models (Van Wassenbergh et al., 2005). In most other cases, however, it has been a challenge to explain the observed variation in scaling trends due to the complicated interplay between size, new morphologies and new behaviors. Here we propose that muscle physiology changes dominate the scaling of whole body kinematics while fin lever arm changes dominate the scaling of fin movements.

Development and morphology

Two ontogenetic functional transitions have been identified by other authors with respect to pectoral fin function in zebrafish, both occurring at an approximate total length of 1.2 cm: slow swimming behavior changes from axial motions coordinated with alternating left–right fin beats to axial undulations only, and resting fin angle increases steadily from 0° to 45° and remains constant at this value after the transition (Thorsen et al., 2004; Thorsen and Hale, 2005). We find that slow swimming out of a routine turn is not present after approximately *FL*=0.9 cm and that certain kinematic variables

also show such a transition at a similar fish length. Turn angle and angular velocity are better described by two linear relationships with a transition point at *FL*=1.18 cm and *FL*=1.16 cm, respectively (Fig. 5A,B), than by a single linear relationship. Both turn angle and angular velocity change from a negative to a slightly positive rate of change after the transition point. These transition points fall near the ontogenetic transition from the larval to the juvenile stages as found in several other species (Gibb et al., 2006; Hale, 1999).

Does this functional development reflect the underlying morphological development? Thorsen and Hale examined the development of the pectoral fin musculature in zebrafish and described the major morphological changes that occur (Thorsen and Hale, 2005). By the time fish have reached a total length of 1.14 cm they have attained adult morphology with individual muscle bundles controlling each fin ray, a more vertically oriented base of the pectoral fins and a set of three adductor and three abductor muscles attaching on the medial and lateral sides of the fin, respectively (Thorsen and Hale, 2005). This morphology should allow fish to finely control the complex shape of the pectoral fins, as observed during maneuvering (Drucker and Lauder, 2003). Although pectoral fin performance as measured from the dorsal view in this study continues to increase past the transition point (Fig. 6C), coordination of motion in all spatial planes could be changing. We noticed that the pectoral fin on the inside of the turn rotates along its proximodistal axis such that the leading edge of the fin is pointing ventrally at maximum rotation. The three-dimensionality of fin motions during maneuvers such as routine turning is worthy of further exploration and will likely help elucidate the ontogenetic patterns we observe here.

Pectoral fins seem to be most involved in powering routine turns in juveniles (Fig. 4B) when maximum fin velocity is in close temporal proximity to maximum angular velocity. In larvae there is a closer correlation between tail velocity and angular velocity (Fig. 4A). The pectoral fins at the larval stage are moving slower than the body, suggesting that it is the tail that is responsible for powering the turn while the pectoral fins do not even resist the hydrodynamic forces experienced by being dragged through the water (Fig. 4A). Adults show a large variation in the temporal patterns of maximum pectoral and caudal fin velocities and head angular velocity. The large variation in this pattern could indicate the high degree of fine maneuvering control by the tail and fins. This control is not, however, afforded by the linear velocity of pectoral fins, since when we plot the difference between the two pectoral fin velocities against the side of turning we do not see the pattern we had predicted (Fig. 8). The absence of a correlation between one pectoral fin moving faster and a turn in the opposite direction exists throughout ontogeny, suggesting that at all stages the three-dimensional motions of the fins in addition to axial bending are what control the direction of turning.

When examining the ontogeny of body curvature, a variable not dependent on fin morphology yet contributing to the mechanics of turning, we found a decreasing linear relationship between curvature and fish fork length (Fig. 5D). The axial skeleton is fully formed and ossified by 1 cm total length (Bird and Mabee, 2003) and thus stiffer, making it more costly, presumably, to routinely bend the body to high curvatures. The same pattern has been observed in the ontogeny of escape turns of other fishes (Gibb et al., 2006; Hale, 1996) Major changes in the physiology of axial musculature that could account for a transition in a variable such as curvature, occur much earlier, between days 1 and 3 post-fertilization, and are therefore unlikely to account for this transition (Buss and Drapeau, 2000; Hernandez, 2000). However, as the trunk becomes an increasingly larger part of a body that has a constant number of myomeres, the size of each myomere relative to body length increases (Felsenfeld et al., 1990). Thus we would expect that for a given muscle strain, more bending would be generated in an adult fish than in a larva. The combination of changes in axial muscle to body length proportion and an increase in three-dimensional fin movement control likely both contribute to the decrease in body curvature over ontogeny.

Turn duration in our experiments increased over ontogeny at a steady rate, not reaching a plateau by the end of the ontogenetic range examined (Fig. 5C). The same pattern was also observed for caudal and pectoral fin linear velocities (Fig. 6B,C). This suggests that the combination of factors affecting these variables, although correlated to size, are not size limited. The variables are also not limited by the discrete morphological changes occurring. The same effect is true for the development of escape response performance in salmonid fishes (Hale, 1996). Zebrafish head velocity remained unchanged over ontogeny (Fig. 6A), adding support to the hypothesis of Hill (Hill, 1950) that maximum linear velocity is independent of body length.

Median fin function was not assessed in this study although we know that the dorsal and anal fins have important functions during maneuvering (Drucker and Lauder, 2005; Standen and Lauder, 2007). Development of median fins is also complete through ossification by total length 0.9 cm (Bird and Mabee, 2003) and a shift in their function during routine turns could also contribute to the ontogenetic patterns we observed.

Behavioral shifts could be an additional factor affecting ontogenetic changes in kinematics. Such shifts are not accounted for in models of isometric growth since the models assume not only constant behavior but also constant functional roles of muscles over ontogeny (Richard and Wainwright, 1995). A change in foraging behavior could be responsible for the negative association between turn angle and body length between *FL*=0.4 and 1.18 cm, or the transition after *FL*=1.18 cm to a positive rate of change. A similar argument can be made for the transition in swimming mode from coordinated axial and pectoral fin movement to only axial undulations during swimming out of a routine turn for fish larger than 0.89 cm. There is evidence of such ontogenetic shifts related to size similarities in resource use to avoid intra- and inter-specific competition in fish communities and the observed kinematic patterns of routine turns could be associated with such shifts (Werner and Gilliam, 1984). Our understanding of the ecological ontogeny of zebrafish in the wild is very limited, although studies addressing questions such as habitat preference are a good starting point (Spence et al., 2006).

Hydrodynamics

The zebrafish in this study experienced Reynolds numbers

from approximately 200 to 1250, a range narrower than the one measured during coasting in a previous study (McHenry and Lauder, 2005) but larger than an earlier study of routine swimming across ontogeny (Fuiman and Webb, 1988). From calculations of drag coefficients during coasting, McHenry and Lauder identify a viscous hydrodynamic regime for $Re<300$, an inertial regime for $Re>1000$ and a hydrodynamically intermediate regime inbetween (McHenry and Lauder, 2005). From our results, zebrafish up to about 0.70 cm experienced a viscous regime during turning, while fish ranging in size from 0.70 to 2.00 cm experienced an intermediate hydrodynamic regime. Only one individual had a mean *Re* higher than 1000 and therefore operated mostly in an inertial regime. This is a range of *Re* similar to that observed in salmonids performing escape turns (Hale, 1996).

Turning angle has previously been interpreted with respect to average Reynolds number (Fuiman and Webb, 1988). The ontogenetic pattern observed by these authors suggested that at low *Re*, below about 25, fish are usually not able to perform turns higher than 63°, but have no such constraint at higher *Re*. We found a similar pattern to Fuiman and Webb (Fuiman and Webb, 1988) in the intermediate *Re* zone (approximately $200<Re<700$), in which fish turned through a wide range of angles, from 26° to 154°, with the range narrowing to a mean of about 70° around $Re=1000$. This is also the *Re* ($Re=1000$) after which the inertial drag coefficient remains constant (McHenry and Lauder, 2006) and the fish's motion is governed primarily by inertial forces.

In conclusion, we find that the ontogeny of kinematic variables describing routine turns of zebrafish show three types of growth trends: a biphasic trend with a transition point when the fish attain adult morphology, a single linear relationship between variable and fish size and a single linear relationship that is size independent. The transition identified for biphasic patterns coincides with morphological transitions from larval to juvenile form and to the transition point identified by the measurement of other variables in previous studies. Complete description of fin function during routine turning will require three-dimensional information to fully capture the motion of the fins. The contribution of this three-dimensional variation as well as of behavioral shifts during ontogeny are likely factors and need to be assessed. We also find that the scaling patterns are not the same for all kinematic variables, as indicated by the varied support for the two scaling models, indicating that the scaling of different variables is dominated by changes in different morphologies. The broader significance and source of the different kinematic ontogenetic scaling patterns identified here will be hard to completely evaluate until we have ecological data on the function and fitness effects of variation in this behavior.

List of symbols and abbreviations

FL	fork length (cm)
H	location of the fish head when body is straight
H′	location of the fish head when body is bent
T	location of the fish tail when body is straight
T′	location of the fish tail when body is bent
α	angle complementary to γ (°)
β	angle subtended by the bent fish body (°)
γ	turn angle (°)
K	curvature (cm^{-1})
R	radius of curvature (cm)

We thank Salvatore J. Sciascia and Jessica Miller for their help with animal care. Emily Standen, Eric Tytell and Peter Madden provided useful Matlab code. Members of the Lauder Lab, Jennifer Nauen, Andrew Carroll and two anonymous reviewers provided helpful comments on the manuscript. This research was supported by NSF grant IBN0316675 to G.V.L.

References

Bird, N. C. and Mabee, P. M. (2003). Developmental morphology of the axial skeleton of the zebrafish, *Danio rerio* (Ostariophysi: Cyprinidae). *Dev. Dyn.* **228**, 337-357.

Budick, S. A. and O'Malley, D. M. (2000). Locomotor repertoire of the larval zebrafish: swimming, turning and prey capture. *J. Exp. Biol.* **203**, 2565-2579.

Buss, R. R. and Drapeau, P. (2000). Physiological properties of zebrafish embryonic red and white muscle fibers during early development. *J. Neurophysiol.* **84**, 1545-1557.

Domenici, P. and Blake, R. W. (1997). The kinematics and performance of fish fast-start swimming. *J. Exp. Biol.* **200**, 1165-1178.

Drapeau, P., Saint-Amant, L., Buss, R. R., Chong, M., McDearmid, J. R. and Brustein, E. (2002). Development of the locomotor network in zebrafish. *Prog. Neurobiol.* **68**, 85-111.

Drucker, E. G. and Lauder, G. V. (2003). Function of pectoral fins in rainbow trout: behavioral repertoire and hydrodynamic forces. *J. Exp. Biol.* **206**, 813-826.

Drucker, E. G. and Lauder, G. V. (2005). Locomotor function of the dorsal fin in rainbow trout: kinematic patterns and hydrodynamic forces. *J. Exp. Biol.* **208**, 4479-4494.

Felsenfeld, A. L., Walker, C., Westerfield, M., Kimmel, C. and Streisinger, G. (1990). Mutations affecting skeletal muscle myofibril structure in the zebrafish. *Development* **108**, 443-459.

Fuiman, L. A. and Webb, P. W. (1988). Ontogeny of routine swimming activity and performance in zebra danios (Teleostei: Cyprinidae). *Anim. Behav.* **36**, 250-261.

Gibb, A. C., Swanson, B. O., Wesp, H., Landels, C. and Liu, C. (2006). Development of the escape response in teleost fishes: do ontogenetic changes enable improved performance? *Physiol. Biochem. Zool.* **79**, 7-19.

Hale, M. E. (1996). The development of fast-start performance in fishes: escape kinematics of the chinook salmon (*Oncorhynchus tshawytscha*). *Am. Zool.* **36**, 695-709.

Hale, M. E. (1999). Locomotor mechanics during early life history: effects of size and ontogeny on fast-start performance of salmonid fishes. *J. Exp. Biol.* **202**, 1465-1479.

Hale, M. E. (2002). S- and C-start escape responses of the muskellunge (*Esox masquinongy*) require alternative neuromotor mechanisms. *J. Exp. Biol.* **205**, 2005-2016.

Hale, M. E., Day, R. D., Thorsen, D. H. and Westneat, M. W. (2006). Pectoral fin coordination and gait transitions in steadily swimming juvenile reef fishes. *J. Exp. Biol.* **209**, 3708-3718.

Harper, D. G. and Blake, R. W. (1989). A critical analysis of the use of high-speed film to determine maximum accelerations of fish. *J. Exp. Biol.* **142**, 465-471.

Hernandez, L. P. (2000). Intraspecific scaling of feeding mechanics in an ontogenetic series of zebrafish, *Danio rerio*. *J. Exp. Biol.* **203**, 3033-3043.

Hill, A. V. (1950). The dimensions of animals and their muscular dynamics. *Sci. Prog.* **38**, 209-230.

Jayne, B. C. and Lauder, G. V. (1995). Speed effects on midline kinematics during steady undulatory swimming of largemouth bass, *Micropterus salmoides*. *J. Exp. Biol.* **198**, 585-602.

Lauder, G. V. and Drucker, E. G. (2004). Morphology and experimental hydrodynamics of fish fin control surfaces. *IEEE J. Oceanic Eng.* **29**, 556-571.

Mabee, P. M., Crotwell, P. L., Bird, N. C. and Burke, A. C. (2002). Evolution of median fin modules in the axial skeleton of fishes. *J. Exp. Zool.* **294**, 77-90.

McHenry, M. J. and Lauder, G. V. (2005). The mechanical scaling of coasting in zebrafish (*Danio rerio*). *J. Exp. Biol.* **208**, 2289-2301.

McHenry, M. J. and Lauder, G. V. (2006). Ontogeny of form and function:

locomotor morphology and drag in zebrafish (*Danio rerio*). *J. Morphol.* **267**, 1099-1109.

Muller, U. K. and van Leeuwen, J. L. (2003). Swimming of larval zebrafish: ontogeny of body waves and implications for locomotory development. *J. Exp. Biol.* **207**, 853-868.

Nauen, J. C. and Shadwick, R. E. (1999). The scaling of acceleratory aquatic locomotion: body size and tail-flip performance of the California spiny lobster *Panulirus interruptus*. *J. Exp. Biol.* **202**, 3181-3193.

Nauen, J. C. and Shadwick, R. E. (2001). The dynamics and scaling of force production during the tail-flip escape response of the California spiny lobster *Panulirus interruptus*. *J. Exp. Biol.* **204**, 1817-1830.

O'Reilly, J. C., Lindstedt, S. L. and Nishikawa, K. C. (1993). The scaling of feeding kinematics in toads (Anura: Bufonidae). *Am. Zool.* **33**, 147.

Richard, B. and Wainwright, P. (1995). Scaling the feeding mechanism of largemouth bass (*Micropterus salmoides*): kinematics of prey capture. *J. Exp. Biol.* **198**, 419-433.

Saint-Amant, L. and Drapeau, P. (1998). Time course of the development of motor behaviors in the zebrafish embryo. *J. Neurobiol.* **37**, 622-632.

Spence, R., Fatema, M. K., Reichard, M., Huq, K. A., Wahab, M. A., Ahmed, Z. F. and Smith, C. (2006). The distribution and habitat preferences of the zebrafish in Bangladesh. *J. Fish Biol.* **69**, 1435-1448.

Standen, E. M. and Lauder, G. V. (2005). Dorsal and anal fin function in bluegill sunfish *Lepomis macrochirus*: three-dimensional kinematics during propulsion and maneuvering. *J. Exp. Biol.* **208**, 2753-2763.

Standen, E. M. and Lauder, G. V. (2007). Hydrodynamic function of dorsal and anal fins in brook trout (*Salvelinus fontinalis*). *J. Exp. Biol.* **210**, 325-339.

Thorsen, D. H. and Hale, M. E. (2005). Development of zebrafish (*Danio rerio*) pectoral fin musculature. *J. Morphol.* **266**, 241-255.

Thorsen, D. H., Cassidy, J. J. and Hale, M. E. (2004). Swimming of larval zebrafish: fin-axis coordination and implications for function and neural control. *J. Exp. Biol.* **207**, 4175-4183.

Toro, E., Herrel, A., Vanhooydonck, B. and Irschick, D. J. (2003). A biomechanical analysis of intra- and interspecific scaling of jumping and morphology in Caribbean Anolis lizards. *J. Exp. Biol.* **206**, 2641-2652.

Tytell, E. D. (2004). Kinematics and hydrodynamics of linear acceleration in eels, *Anguilla rostrata*. *Proc. R. Soc. Lond. B Biol. Sci.* **271**, 2535-2540.

Van Wassenbergh, S., Aerts, P. and Herrel, A. (2005). Scaling of suction-feeding kinematics and dynamics in the African catfish, *Clarias gariepinus*. *J. Exp. Biol.* **208**, 2103-2114.

Wakeling, J. M. (2006). Fast-start mechanics. In *Fish Biomechanics: Fish Physiology*, *Vol. 23* (ed. R. E. Shadwick and G. V. Lauder), pp. 333-368. San Diego: Academic Press.

Webb, P. W. (1993). Swimming. In *Physiology of Fishes* (ed. D. H. Evans), pp. 47-73. Boca Raton, FL: CRC Press.

Webb, P. W. and Weihs, D. (1986). Functional locomotor morphology of early life-history stages of fishes. *Trans. Am. Fish. Soc.* **115**, 115-127.

Werner, E. E. and Gilliam, J. F. (1984). The ontogenetic niche and species interactions in size structured populations. *Annu. Rev. Ecol. Syst.* **15**, 393-425.